energies

MDPI

Article

Testing the Stability of NASICON Solid Electrolyte in Seawater Batteries †

Mihaela Iordache, Anisoara Oubraham *, Simona Borta, George Ungureanu and Adriana Marinoiu

National R&D Institute for Cryogenics and Isotopic Technologies—ICSI Ramnicu Valcea, Uzinei No. 4, 240050 Vâlcea, Romania; mihaela.iordache@icsi.ro (M.I.); simona.borta@icsi.ro (S.B.); george.ungureanu@icsi.ro (G.U.); adriana.marinoiu@icsi.ro (A.M.)

* Correspondence: anisoara.oubraham@icsi.ro

† This paper is an extended version of our paper published in 16th International Conference on Electronics, Computers and Artificial Intelligence (ECAI), Iasi, Romania, 27–28 June 2024; pp. 1–6.

Abstract: Rechargeable batteries play a crucial role in the utilization of renewable energy sources. Energy storage systems (ESSs) are designed to store renewable energy efficiently for immediate use. The market for energy storage systems heavily relies on lithium-ion batteries due to their high energy density, capacity, and competitiveness. However, the increasing cost and limited availability of lithium make long-term use challenging. As an alternative to Li-ion batteries, rechargeable seawater batteries are gaining attention due to their abundant and complementary sodium ion active materials. This study focuses on the preparation and characterization of $Na_{3.0}Zr_2Si_2PO_{12}$- and $Na_{3.15}Zr_2Si_2PO_{12}$-type ceramic membranes and testing their stability in seawater batteries used as solid electrolyte. From the surface analysis, it was observed that the $Na_{3.15}Zr_2Si_2PO_{12}$ powder showed a specific surface area of 2.94 m^2/g compared to 2.69 m^2/g for the $Na_{3.0}Zr_2Si_2PO_{12}$ powder. The measured NASICON samples achieved ionic conductivities between 7.42×10^{-5} and 4.4×10^{-4} S/cm compared to the NASICON commercial membrane with an ionic conductivity of 3.9×10^{-4} S/cm. Battery testing involved charging/discharging at various constant current values (0.6–2.0 mA), using Pt/C as the catalyst and seawater as the catholyte.

Keywords: seawater batteries; NASICON ceramic membrane; electrochemical cell

check for updates

Citation: Iordache, M.; Oubraham, A.; Borta, S.; Ungureanu, G.; Marinoiu, A. Testing the Stability of NASICON Solid Electrolyte in Seawater Batteries. *Energies* **2024**, *17*, 5241. https://doi.org/10.3390/en17215241

Academic Editor: Oscar Barambones

Received: 25 September 2024
Revised: 16 October 2024
Accepted: 18 October 2024
Published: 22 October 2024

Copyright: © 2024 by the authors. Licensee MDPI, Basel, Switzerland. This article is an open access article distributed under the terms and conditions of the Creative Commons Attribution (CC BY) license (https://creativecommons.org/licenses/by/4.0/).

1. Introduction

In order to preserve a sustainable and clean global ecosystem, today's society faces the need for decarbonization and the reduction of carbon dioxide emissions [1]. These carbon dioxide (CO_2) emissions that lead to global warming, emissions with a greenhouse effect, result from obtaining energy based on non-renewable sources of fossil fuels. The promotion of "zero emission" stocks like renewable energy sources (RES) is driven by the need to reduce carbon dioxide and pollutants. In the future, energy storage systems (ESSs) will be crucial in addressing the uncertainty and intermittency of renewable energy sources. ESS offers high scalability, flexibility, efficiency, and rapid response, making it an efficient, sustainable, economical, and safe solution for electricity supply. ESS can be classified into five main categories: chemical energy storage, electrochemical energy storage, electrical energy storage, mechanical energy storage, and thermal energy storage [2]. Thus, the aim is to obtain clean and sustainable energy, with reduced emissions in terms of greenhouse gases [3]. Renewable or green energy obtained from natural sources, whether we are talking about sunlight, water flows, wind, or even waves, does not affect the environment in a negative way, such as by eliminating greenhouse gases in the atmosphere. Green energy will certainly replace fossil fuels, as this is crucial if we want to achieve our climate goals, but this will require significant investment, and each country and region will have to figure out what is the most efficient type of green energy that it can implement. Also, through methods of physical capture and chemical conversion, attempts are made to reduce the

CO_2 content in the atmosphere [4]. Over time, technology advances, and as we implement as many green energy sources as possible, its will be able to provide us with the energy we need, without having a negative impact on the environment compared to fossil fuels. As technology develops, this will change, but currently, wind turbines seem to be the most efficient, as compared to solar panels, they need the least refining and processing. Also, they require less maintenance and are not affected by cloudy or gloomy weather. Conversely, wind turbines can generate more power the gloomier the weather and the stronger the wind, up to a point. The three types of green energy sources, wind energy, geothermal energy, and hydro energy, are currently the most efficient and easy to exploit, and the advantage offered by geothermal energy and hydro energy is that they have been used for a long time, which has allowed for a longer period of development and research. Hydropower also has great potential when it comes to the amount of energy it can deliver to more households. Along with the development of renewable energy sources, the development of a cost-effective electricity storage system and its transformation into a practical electrical source is also being pursued. This problem can be solved by using as an electrochemical storage medium called a battery or electrical components that store the electrical charge in the form of a potential difference called capacitors [5]. Also, mechanical, electromagnetic, electrochemical, and thermochemical technologies represent renewable energy storage solutions. Considering the development and use of lithium-ion type batteries, problems related to several factors, such as their safety (type of electrolytes), the price of the battery's component elements, and the method of recycling batteries, still continue to exist. Looking at these problems, a new type of battery, sea water batteries, is given a lot of attention [6]. These batteries use, as their name implies, natural sea water as an aqueous chemical electrolyte. Compared to lithium-ion batteries, seawater batteries present great factors of safety, price, compatibility, the reduction of fresh water consumption, and durability. The uniqueness of the physical and chemical properties of sea water is given by its salt content. Thus, the stable constituents of sea water are a neutral pH and ionic conductivity, regardless of the collection area of this water.

The 3.5% salt content of seawater gives it unique physical and chemical properties, making it a suitable natural resource for use as an electrolyte in ESS devices. Seawater-based batteries (SWBs) not only help conserve precious freshwater resources by replacing fresh water with seawater but also reduce the cost of electrolytes and overall battery systems. As a result, SWBs offer a safer, more economical, and environmentally friendly alternative to other aqueous batteries that use fresh water as an electrolyte [7].

The Mg/AgCl batteries were the initial batteries to use seawater for activation. In 1949, Mg/CuCl batteries were first introduced, followed by Mg/$PbCl_2$, Mg/$HgCl_2$, Mg/PbO_2, Mg/PbO_2, and Al/AgO batteries, all of them being commercially and civilly used. Mg-DO (Mg-dissolved oxygen) batteries and Al-seawater-activated batteries were created to meet the demands of deep-sea applications and long-term subsea work in the late 20th century due to their high energy densities. SWBs, including Na-air, Zn-air, Na-ion, and Cl-ion, have been created with various working mechanisms and electrode materials, including metal, polymers, carbon materials, and nanomaterials. Exploring design strategies to create an energy storage solution that is efficient, reusable, and durable for various applications is taking place. The objective of these strategies is to tackle challenges such as safety problems, low energy density compared to lithium-ion batteries, the nature of seawater, and the selection of electrode materials [7].

In order to improve battery performance, it is crucial to thoroughly study the mechanism and all components of the battery. The rapid development of $MeCO_2$ (Metal-CO_2) batteries can be hindered due to the slow kinetics of electrode reactions. This comprehensive review of $MeCO_2$ batteries offers a detailed discussion of all aspects of $MeCO_2$ battery research. It covers the study of battery reaction mechanisms, cathode catalyst structures, types of electrolytes, and metal anodes. This not only aids researchers in understanding $MeCO_2$ batteries but also serves as a reference for their development [4].

Due to the similar chemical properties of sodium and lithium, there has been a growing interest in researching sodium-based rechargeable batteries. Both sodium and lithium are group 1 elements with comparable standard potentials of the electrode, which determines some of the battery potential (−2.71 V for Na^+ and −3.04 V for Li^+). As a result, sodium ion batteries (SIBs) have been widely studied as alternative energy storage (ESS) technologies. Comparing the costs of these two types of batteries, it was observed that SIBs are considerably cheaper than lithium-ion batteries (LIBs), with a 12.5% cost reduction caused by the lower price of sodium materials. The potential of SIBs has been enhanced by the development of rechargeable batteries with seawater (SWB) due to the affordability of cathode and catholic materials. SWBs, which are essentially sodium metal batteries, can directly extract Na^+ from seawater to store energy. SWBs are more energy dense than LIB (4010 Wh/kg for SWB vs. 568 Wh/kg for LIB) and can produce fresh water by desalinating seawater during the loading process. The use of seawater as a catholite is highly advanced, as it can reduce the total cost of ESS and increase the theoretical volumetric energy density compared to LIB (3051 Wh/L for SWBs vs. 1901 Wh/L for LIB). It is expected that SWBs with high volumetric and gravimetric energy densities will simplify the spatial requirements of ESS at a large scale and lower the weight of electric vehicles. Although there are potential advantages, the exploration of SWBs for renewable energy storage has not been detailed because they are still in the early stages of development [1]. A new, affordable, and environmentally friendly rechargeable battery has been developed, using seawater, which is abundant in nature, as an activation material [8–10]. The super-concentrated electrolytes used in these batteries are called 'water-in-salt (WiS) electrolytes' because of their wide electrochemical stability, cost-effectiveness, and non-flammability. However, the highly reactive nature of the alkali metals Li and Na prevents the direct use of WiS electrolytes, but using a ceramic separator to separate the anode and cathode during the discharge-charge process allows the successful use of Na-CO_2 batteries based on WiS electrolytes [11–13]. The electrochemical cell to be tested consists of an anode and a cathode, separated by a solid electrolyte of the sodium superionic conductor (NASICON) type ($Na_3Zr_2Si_2PO_{12}$) [9].

High ionic conductivity and relatively high chemical stability are characteristics of NASICON (Na super ionic conductors). The suggestion is to use this material as a solid electrotrolyte in solid-state electrochemical devices like gas sensors, ion sensors, and Na batteries [14–16]. $Na_3Zr_2Si_2PO_{12}$ (NZSP) was first proposed by Hong and Goodenough in 1976 and is considered to be the most effective ionic conductivity among $Na_{1+x}Zr_2Si_2P_{3-x}O_{12}$ materials for x = 2 [17–22]. The structure of $Na_{1+x}Zr_xSi_2P_{3-x}O_{12}$ can be described as a three-dimensional network of ZrO_6 octahedra sharing corners with PO_4/SiO_4 tetrahedra. Na^+ ions can be found in the interstitial sites within this framework. Silicate and phosphate tetrahedral structures share six oxygen molecules with their counterparts, ZrO_6 octahedral structure. Each tetrahedral and octahedral component is connected by oxygen molecules. Repeating structures are created along the c-axis this way. The primary way to transport Na^+ ions is by moving them through holes (known as 'bottlenecks') in the 3D structure, which are interstitial sites between octahedral and tetrahedral structures. Ionic diffusion is influenced by the size of the bottleneck area as Na^+ ions migrate through bottleneck sites based on their activation energies (hopping mechanism) [23,24]. NZSP is viewed as an exciting solid-state electrolyte material for sodium batteries. NZSP's interfacial resistance has been reduced through various efforts to improve its ionic conductivity and achieve good performance at room temperature. A solid electrolyte structured with NASICON $Na_{3.1}Zr_{1.95}Mg_{0.05}Si_2PO_{12}$ was synthesized using a simple solid-state reaction. This process resulted in a high sodium-ionic conductivity of 1.33×10^{-3} S/cm at room temperature. Solid-state batteries were then assembled using $Na_{3.1}Zr_{1.95}Mg_{0.05}Si_2PO_{12}$ as the electrolyte, and they maintained a specific capacity of 57.9 mAh/g after 100 cycles under a current density of 0.5 C at room temperature [25]. Initial electrochemical performance tests of solid-state Na-S cells at 60 °C (Na||NZSP||S cell) showed an initial capacity of 136 mAh/g at 10 mA/g, while

a discharge capacity of 76.8 mAh/g was obtained when tested at 20 mA/g [26]. The operation of graphite-based potassium ion batteries (Gr-PIBs) remains challenging at low temperatures due to slow dynamic behavior. However, a dual-tuning strategy of the electrolyte solvation structure is proposed for the multidimensional process improvement of K^+ transfer, including both bulk and interface ion transfer [27,28].

NASICON ceramic membrane batteries have been found to have a long lifespan, with their surface morphology and ion conductivity remaining stable even after 600 test cycles or more than 5 months of seawater immersion tests. These batteries use natural seawater as an active material to charge and discharge, making them suitable for various marine sectors and typical energy storage applications as primary or secondary energy sources. Seawater batteries (SWB) offer a promising energy storage system for the future due to the environmental impact of abundant seawater as an inexpensive source of active Na-ion cathode materials. They use the oxygen evolution reaction (OER) upon charging and the oxygen reduction reaction (ORR) upon discharge, both of which occur on the current collector submerged in high water on the side of the cathode [10,29]. Rechargeable seawater batteries are considered sustainable alternatives to Li-ion batteries due to the unlimited and free supply of Na-ion active materials. Despite the improvements made to seawater batteries, such as the introduction of new catalysts, there is still a need to reconsider the cell design in order to improve performance and increase practical battery production [9,30–32].

The purpose of this study is to determine the stability of a battery containing a NASICON ceramic membrane as solid electrolyte with metallic Na as anode. Charge/discharge testing was conducted at various constant current values using Pt/C as a catalyst and seawater as the catholyte.

2. Materials and Methods

2.1. Preparing Membranes $Na_{3.0}Zr_2Si_2PO_{12}$ (NAS) and $Na_{3.15}Zr_2Si_2PO_{12}$ (NAS-5%)

The NAS and NAS-5% membranes were created through a solid-state reaction process. This involved mixing Na_2CO_3 (Alfa Aesar, Haverhill, MA, USA), SiO_2 (Umicore), ZrO_2 (Sigma-Aldrich, Saint Louis, MO, USA), and $NH_4H_2PO_4$ (Scharlab, Barcelona, Spania) in the stoichiometric ratio Na:Zr:Si:P = 3.0:2.0:2.0:1.0 and 3.15:2.0:2.0:1, respectively. The raw materials were mixed for 8 h by ball milling with ZrO_2 balls of 3 mm, 5 mm, and 10 mm diameter, along with ethanolic solvent, at 300 rpm in a ZrO_2 container. The obtained mixture was then dried at 80 °C. After preheating at 600 °C for 4 h, the powder was then calcined at 1100 °C for another 4 h. The calcined powder was ground for 4 h by ball milling at 500 rpm using ZrO_2 balls with a diameter of 3 mm and ethanolic solvent, and the obtained mixture was dried at 80 °C. The powder obtained by NASICON was pressed in a hydraulic press by cold isostatic pressing at different pressing forces (between 2500 and 3500 KgF/cm^2) for 5 min to form pellets of approximately 20 mm diameter and 1.0 mm thickness. The obtained pellets were placed in an alumina crucible, on their clean powder to avoid contamination, and placed in the furnace for sintering. Sintered pellets were made from fabricated material at temperatures of 1100 °C and 1150 °C for 10 h, with a heating rate of 5 °C/min, in nitrogen gas in a tube furnace to eliminate volatile species (Figure 1). The laboratory pellets were compared with a standard commercial NASICON membrane (NZSP, 4TOONE Ltd., Ulsan, Republic of Korea) [33].

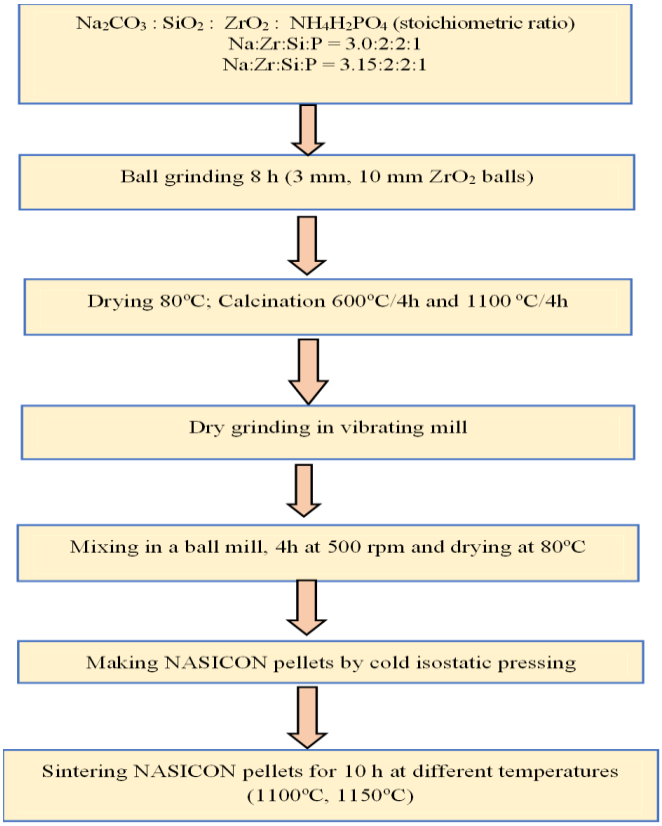


Figure 1. Techniques to obtain the NASICON membrane, both with and without excess sodium. 5%.

2.2. Membrane Characterization Equipment and Methods

The BET (Brunauer-Emett-Teller) technique was employed to determine specific surface area using an Autosorb IQ analyzer (Quantachrome, Boynton Beach, FL, USA). The nitrogen adsorption-desorption was executed at 77 K and the samples were subjected to degassing at 115 °C for 4–6 h before the analysis. The pore size distribution was assessed using the Barrett-Joyner-Halenda (BJH) method and the desorption isotherm equations. The crystal structure of the NASICON samples was analyzed using X-ray diffraction (XRD) with a Rigaku MiniFlex 600 X-Ray diffractometer (Tokyo , Japan) equipped with a CuK-a X-ray source (wavelength 1.541838 Å). To reduce noise levels, a monochromator was utilized to conduct scans from 10° to 60° at high resolution (with a scanning step of 0.01° and scan speed of 1.0° min^{-1}). Broadband conductivity measurements were carried out using a Novocontrol Concept 40 high-resolution analyzer across a frequency range from 10^{-1} to 10^{7} Hz and a temperature range from −100 °C to 100 °C. The Quattro Cryosystem temperature controller, which has a temperature stability of more than 0.1 K, was used in a dry nitrogen atmosphere. Measurement of conductivity was conducted isothermally using 10K steps with an AC voltage amplitude of 0.1 V. Before each measurement, the samples were annealed in the Novocontrol cell at 120 °C in a stream of nitrogen for 2 h to eliminate any moisture acquired during loading and solvent preparation.

2.3. Obtaining the Battery That Contains the NASICON Membrane (The Anode Compartment)

To assemble the battery (the anode compartment), we worked in a glove box with a high-purity Ar atmosphere where oxygen and water levels were below 1.0 ppm. We used a NASICON membrane with a thickness of approximately 1 mm and a diameter of around 20 mm as a solid electrolyte. This membrane was placed on the top round and perforated cover that holds the anode compartment. Sodium metal (purity 99.9%, Sigma Aldrich) was attached to the surface of a stainless-steel separator that was used as an anodic current collector. To separate metallic Na from the NASICON membrane, we used a polyethylene

separator 16 µm thick and about 18 mm in diameter over which an organic electrolyte (about 50 µL) of 1 M sodium trifluoromethanesulfonate ($NaCF_3SO_3$, Sigma-Aldrich Co.) in tetraethylene glycol dimethyl ether (TEGDME, Sigma-Aldrich Co.) was placed. To tightly push the compartment inside the SWB, a metal spring was utilized. We used an adjustable assembly mechanism/roller seal to secure the SWB compartments and prevent organic electrolyte leakage and infiltration by assembling the battery that contained a NASICON ceramic membrane, as seen in Figure 2.

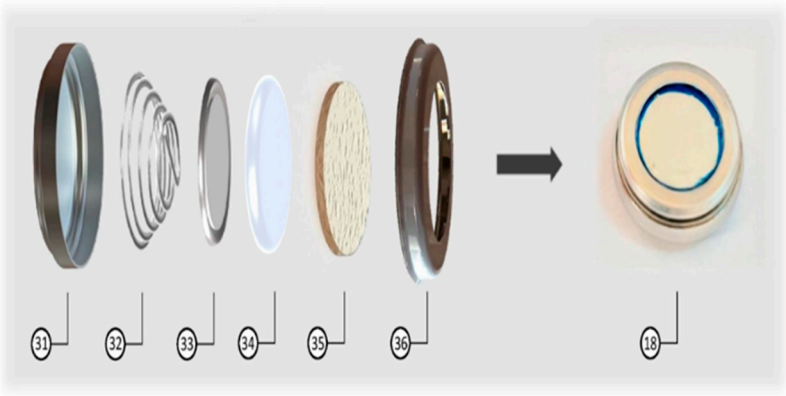


Figure 2. The components of the NASICON ceramic membrane battery: (31) lower part of the battery; (32) compression spring; (33) sodium (Na) metal; (34) organic electrolyte; (35) NASICON membrane; (36) top of battery; (18) NASICON membrane battery [34].

2.4. Preparation of the Catalytic Mixture and the Cathode

The catalyst mixture was prepared in a catalytic ink by dispersing 0.025 g of 40% Pt/C catalyst (Thermo Scientific, Ward Hill, MA, USA) in 1.3 mL of binder solution. The binder solution consisted of 0.3 mL Nafion D-521 dispersion (5% *w*/*w* in water and 1-propanol), 0.25 mL distilled water, and 0.75 mL 2-propanol (99+%, Thermo Scientific, Ward Hill, MA, USA). The mixture was then sonicated for 2 h. The cathode was prepared by spraying 50 µL of catalytic ink (Pt/C ink) onto a carbon felt electrode, with a charge density of 0.00031 g Pt/cm^{-2}. The carbon felt that was coated with catalytic ink was heated in an oven at 80 °C for 3 h. The carbon sheet coated with Pt/C (0.00031 g Pt/cm^2) was used as a cathodic current collector.

3. Results and Discussion

3.1. Characterization of the Structure of NASICON Membranes

Identifying particle properties requires understanding particle size and distribution. Smaller particle sizes generally lead to better ionic conductivity, and the size of particles has a significant impact on the conductivity of crystalline electrolytes. In Figure 3, it is shown that 10% of the NASICON particles sintered at 1100 °C have a size of approximately 1000 nm, while for NASICON sintered at 1150 °C, the particles have a size ranging between 618.6 and 1315.4 nm. D_m represents the modal diameter of the distributions, and D_{50} represents the median. The data indicate that the texture of the NASICON composition is directly influenced by the high sintering temperature.

After sintering the NASICON materials, we conducted an XRD analysis to examine their crystalline structure (see Figure 4). We compared the laboratory-prepared samples with a commercial NASICON sample. By referencing the literature for NASICON materials of the same composition [35], we identified the Miller crystallographic indices corresponding to primary NASICON signatures. We found that the peaks of lower intensity corresponded to zirconium phases. The primary NASICON phases showed high crystallinity in the sintered samples, with interplanar spacing d increasing with increasing 2θ angles. Most NASICON phases had a maximum crystallite size of less than 100 nm. The primary NASICON peak restoration in the sintered samples was consistent with the

spectra from the commercial control sample. Traces of monoclinic ZrO_2 were detected after sintering, which was caused by the volatilization of P and Na from NASICON during calcination. The density calculations were compared to the literature's results, with 3.27 g/cm^3 for $Na_3Si_2Zr_2PO_{12}$. NAS and NAS 5% pellets recorded density values of 3.218 g/cm^3 and 3.229 g/cm^3, respectively.

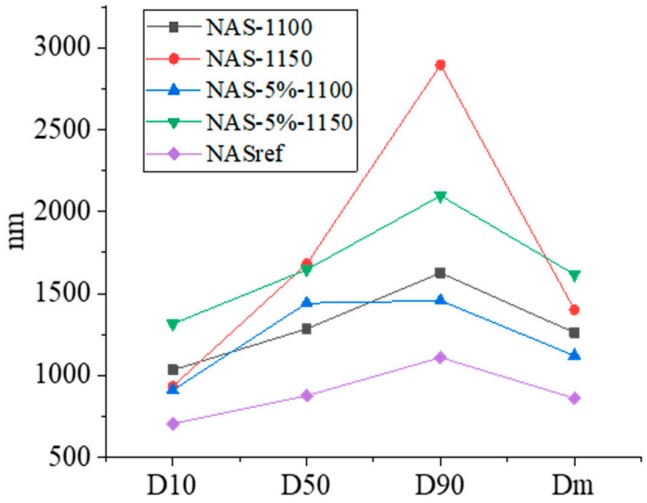


Figure 3. The distribution of particle sizes in NASICON membranes.

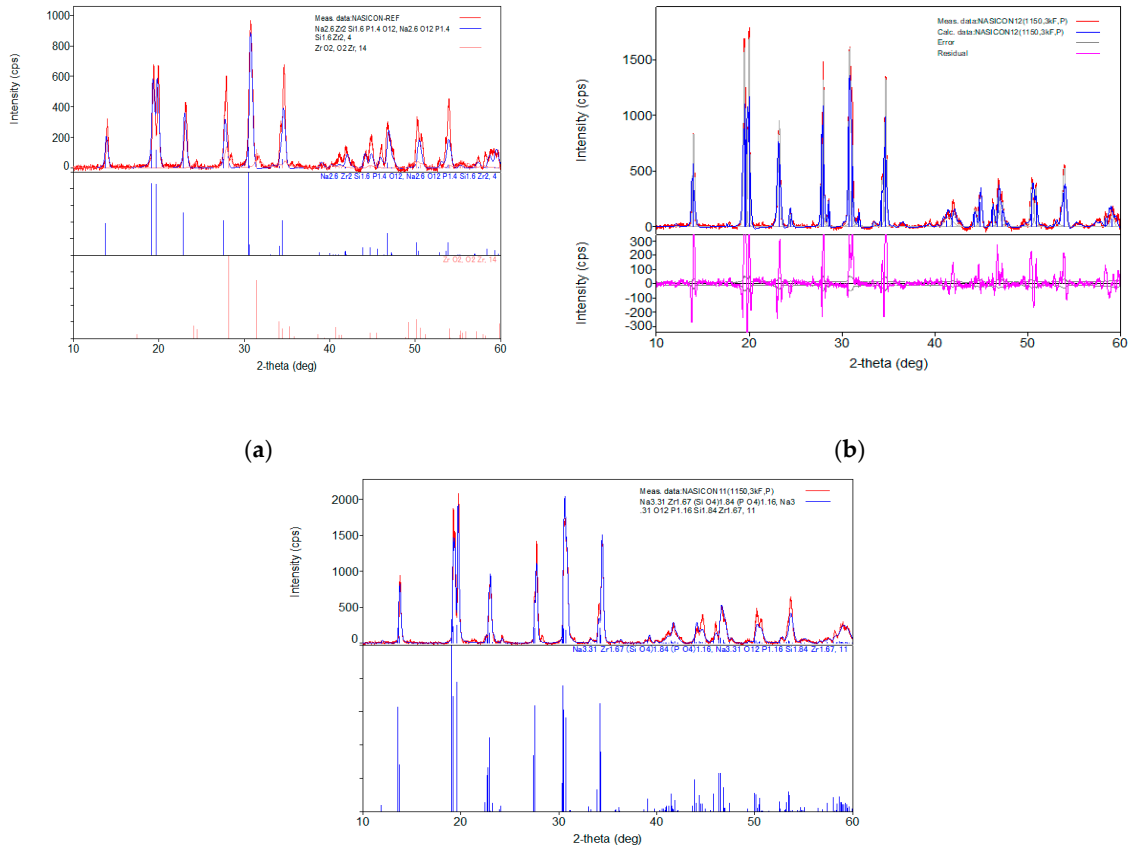
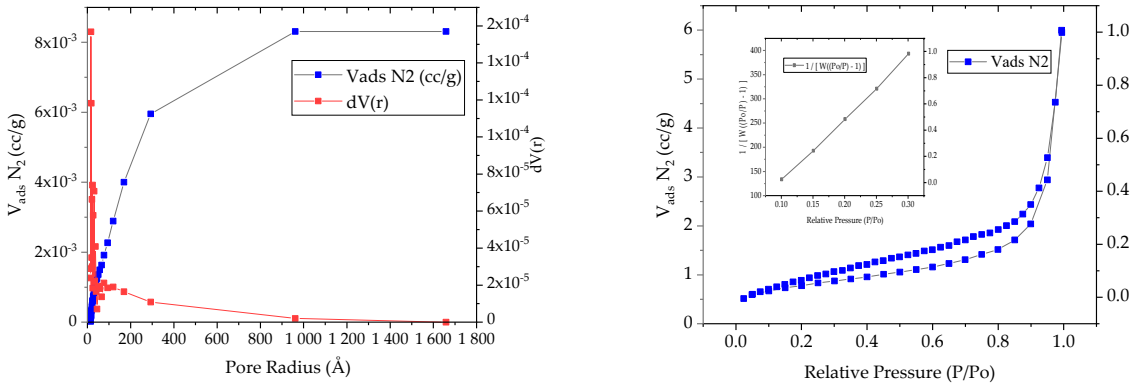


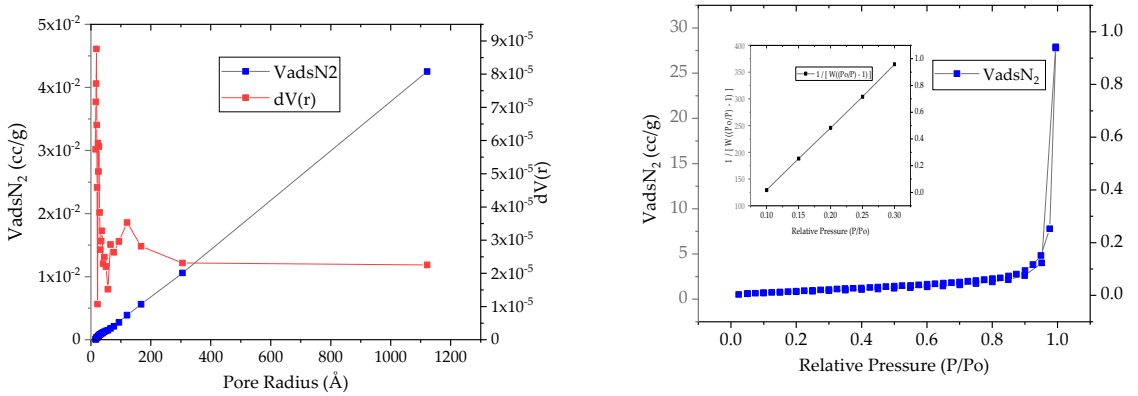
Figure 4. XRD spectra of NASICON materials: (**a**) NASICON commercial reference sample; (**b**) NASICON pressed at 3000 kgF/cm^2 and sintered at 1150 °C; (**c**) NASICON with an excess of 5% Na, pressed at 3000 kgF/cm^2 and sintered at 1150 °C.

The NASICON samples were analyzed using BET and BJH analysis to examine their surface and microporosity. The results are available in Figures 5 and 6. The specific surface area can be determined by measuring the amount of gas N_2 that has adsorbed or desorbed from the surface of porous solids with the static (volumetric) manometric method. The predominance of a mesoporous structure can be seen in the hysteresis loop observed in both admisorption and desorption isotherms. Differences in interface geometry between adsorption and desorption result in hysteresis. The BJH textural analysis results can be found in Table 1. According to surface analysis, NASICON powder with 5% excess had a specific surface area of 2.94 m^2/g, while NASICON powder without excess Na had a specific surface area of 2.69 m^2/g.



(**a**) (**b**)

Figure 5. BET (**a**) and BJH (**b**) of the surface porosity of NASICON powder without excess of Na was evaluated.



(**a**) (**b**)

Figure 6. BET (**a**) and BJH (**b**) of the surface porosity of NASICON powder with an excess of Na of 5% was evaluated.

Table 1. Analyzing the specific surface area and porosity of NASICON powder using the BET method and the BJH method.

Sample	Specific Surface Area (m^2/g)	Pore Volume (cc/g)	Average Pore Radius (Å)
NASICON pre-sintered powder without excess Na	2.69	0.008	16.55
NASICON pre-sintered powder with excess Na 5%	2.94	0.043	18.52

3.2. Testing the Electrical Properties of NASICON Membrane

The logarithmic scale on both axes is used to display the ionic conductivity values for NASICON membranes, which are shown as a function of frequency at room temperature (RT) in Figure 7. The measured NASICON samples showed ionic conductivities ranging between 7.42×10^{-5} (NAS 1100) and 2.43×10^{-4} S/cm (NAS 5% 1100) for the samples sintered at 1100 °C, and between 1.55×10^{-4} and 4.4×10^{-4} S/cm for samples sintered at 1150 °C. For comparison, a commercial NASICON membrane (NAS Ref) displayed an ionic conductivity of 3.9×10^{-4} S/cm. The NASICON sample with 5% excess sintered at 1150 °C exhibited a higher ionic conductivity value compared to the commercial sample, according to the experimental data analysis. Moreover, it was observed that increasing the sintering temperature resulted in a higher ionic conductivity of the membranes. NAS 5% membrane battery testing at 1150 °C in seawater rechargeable battery was carried out at different currents: 0.6, 0.8, 1.0, 1.2, 1.4, 1.6, 1.8, and 2.0 mA and an operating time of approximately 20 h. From the charge/discharge curves, potential values between 3.45 and 3.8 V and an accumulated energy per discharge of 31.9 mWh to 116.7 mWh were obtained (Table 2).

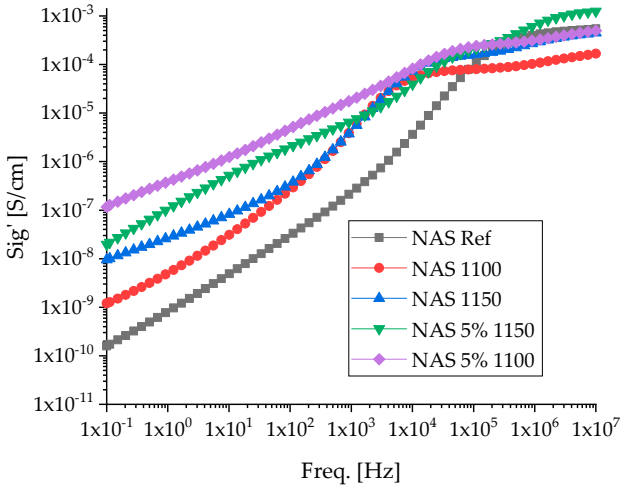


Figure 7. Room temperature (RT) conductivity of NASICON membranes, NSICON reference (NAS Ref), without excess Na (NAS 1100 and NAS 1150), and with 5% excess Na (NAS 5% 1100 and NAS 5% 1150), at different sintering temperature.

Table 2. Technical characteristics of the battery containing NASICON type ceramic membrane using Pt/C catalyst (0.00067 gPt) after approximately 20 h of operation.

Current (mA)	Time (h)		Potential vs. Na/Na^+ (V)		Power (mW)		Energy (mWh)		Capacity (mAh)	
	Charging	Discharge	Charging	Discharge	Charging	Discharge	Charging	Discharge	Charging	Discharge
0.6	21.0	21.0	3.45	2.95	2.07	1.77	43.4	31.9	0.596	0.596
0.8	19.0	20.0	3.57	2.97	2.85	2.37	54.0	47.9	0.795	0.794
1.0	22.0	22.0	3.59	2.85	3.58	2.85	75.3	62.7	0.993	0.993
1.2	21.0	22.0	3.67	2.80	4.40	3.36	91.5	73.0	1.190	1.173
1.4	22.0	22.0	3.77	2.80	5.30	3.92	115.2	81.7	1.398	1.327
1.6	21.0	20.0	3.88	2.95	6.20	4.13	130.0	82.6	1.589	1.390
1.8	21.0	22.0	3.74	2.74	6.73	4.93	141.0	108.5	1.788	1.788
2.0	22.0	22.0	3.77	2.66	7.60	5.30	159.5	116.7	1.987	1.987

3.3. Seawater Battery Performance Testing

The redox electrochemical reactions of hybrid sodium ion migration batteries are almost exclusively powered by the high concentration of Na+ in seawater. Energy storage is primarily achieved by introducing and extracting Na^+ ions into cathode materials in these batteries, a process that is similar to the movement of ions between the anode and cathode in traditional metal ion battery systems. The capacitance of electrode materials is the main factor that determines the electrochemical performance of Na ion migration hybrid batteries, and it is regulated by their Na^+ ion storage mechanisms. Furthermore, these systems frequently utilize Na-ion inserting materials [6]. Solid sodium ion conductive ceramic membranes have led to the popularity of using sodium metal anodes in hybrid batteries. They are preferred because they do not reacquire changes to the seawater electrolyte, and the metallic sodium electrode can naturally form redox couples with the sodium ions abundant in seawater, benefiting from a reduced redox potential of −2.71 V. Ceramic material is very stable in seawater, and its robust structure effectively separates water from active metals. Metal sodium anodes are used in these batteries to operate at high temperatures and voltages up to 4 V, which is considerably higher than those using other metal anodes, like magnesium or zinc. The application of these batteries is enhanced by this [6].

The performance of the battery was tested using a NASICON ceramic membrane as a solid electrolyte in an electrochemical cell with a capacity of 1.5 L (see Figure 8). The testing involved a seawater electrochemical cell with a concentration of about 20 g NaCl/L and CO_2 bubbling at a flow rate of 0.2 L/min for charge/discharge testing of the solid electrolyte battery. To evaluate how well the charge and discharge performs, a two-electrode system was put in place with a metal sodium anode and a carbon felt cathode.

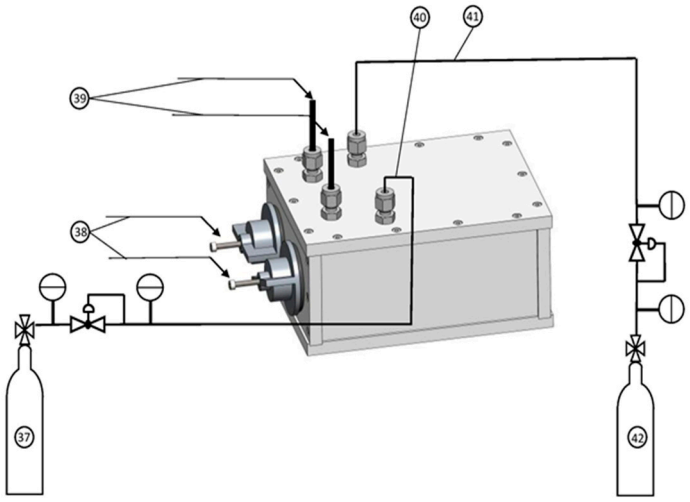


Figure 8. The NASICON ceramic membrane battery electrochemical cell test stack: (37) CO_2 cylinder; (38) anode current collector; (39) cathode current collector; (40) CO_2 feeding route; (41) evacuation route H_2; (42) H_2 cylinder.

Two batteries with NASICON membrane were placed in parallel. The carbon sheet coated with Pt/C (0.00031 g Pt/cm^2) was used as a cathodic current collector, and different currents (0.6, 0.8, 1.0, 1.2, 1.4, 1.6, 1.8, and 2.0 mA, respectively) were applied. Each cycle lasted for 1 h. The mechanism of CO_2 dissolution is described by chemical reactions [34]:

$$CO_2 + H_2O \leftrightarrow H_2CO_3 \quad (1)$$

$$H_2CO_3 \leftrightarrow HCO_3^- + H^+ \quad (2)$$

Metallic sodium's anodic oxidation reaction (3) and cathodic hydrogen release reaction (4) are both part of electrochemical reactions.

$$\text{Anode}: \ 2Na \rightarrow 2Na^{+} + 2e^{-} \quad (3)$$

$$\text{Cathode}: \ 2H^{+} + 2e^{-} \rightarrow H_2 \quad (4)$$

$$\text{Net reaction}: \ 2Na^{+} + 2H^{+} \rightarrow 2Na^{+} + H_2 \quad (5)$$

The graphs from Figures 9–12 display the charge/discharge curves for potential, power, energy, and capacity at various currents: 0.6, 0.8, 1.0, 1.2, 1.4, 1.6, 1.8, and 2.0 mA. Each cycle lasted 1 h, and the total operating time was approximately 20 h. In the potential curves, an increase in potential is evident during charging with higher applied currents. For instance, at a current of 0.6 mA, a potential of 3.45 V was achieved, while at 2.0 mA, the potential reached 3.77 V. An exception was observed at 1.6 mA, where the potential was 3.88 V. During discharge, the potential decreased with higher applied currents, except at 1.2 and 1.4 mA, where identical values were recorded. A potential difference ranging from 0.5 to 1.1 V was also observed, and it was noted that higher applied currents resulted in a greater potential difference. After approximately 20 h of operation, the voltage efficiency during charge/discharge was as follows: 85.5% (0.6 mA), 83.0% (0.8 mA), 79.4% (1.0 mA), 76.3% (1.2 mA), 74.3% (1.4 mA), 76.0% (1.6 mA), 73.3% (1.8 mA), and 71.0% (2.0 mA). It is evident that voltage efficiency decreases with higher applied currents. The battery power obtained per charge ranged from 2.07 to 7.60 mW, while the power obtained per discharge ranged from 1.77 to 5.30 mW. Analysis of the energy curves revealed that the accumulated energy increases with the applied current. The energy accumulated during charging ranged from 43.4 mWh at a current of 0.6 mA to 159.5 mWh at a current of 2.0 mA. During discharge, the values ranged from 31.9 mWh at a current of 0.6 mA to 116.7 mWh at a current of 2.0 mA (Table 2).

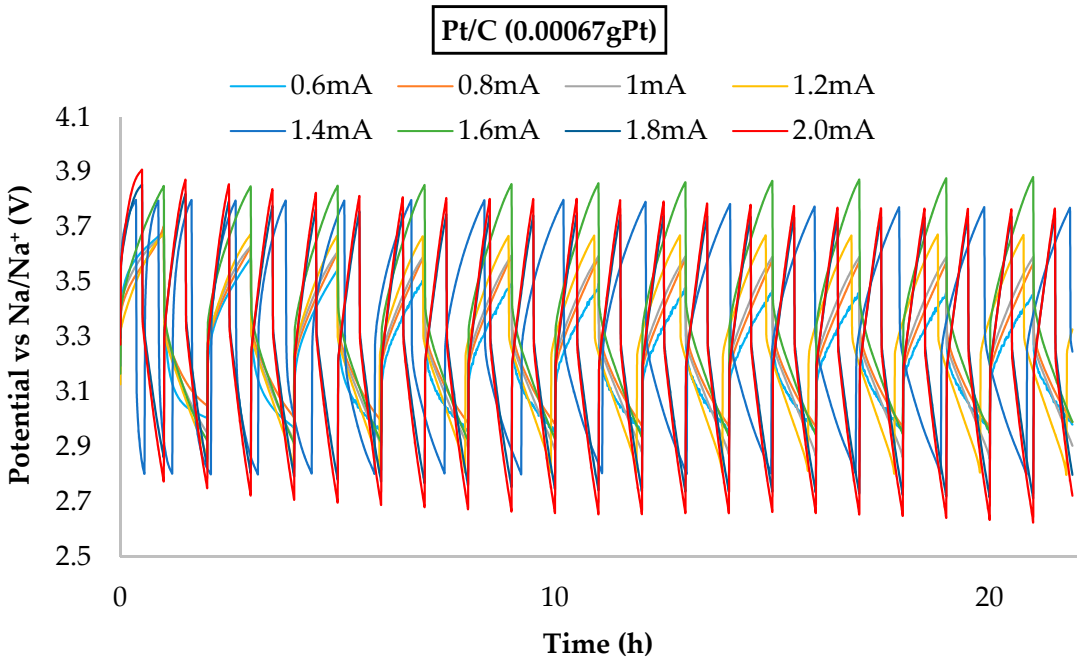


Figure 9. Time evolution of the potential obtained after testing the NASICON membrane battery at currents of 0.6, 0.8, 1.0, 1.2, 1.4, 1.6, 1.8, and 2.0 mA.

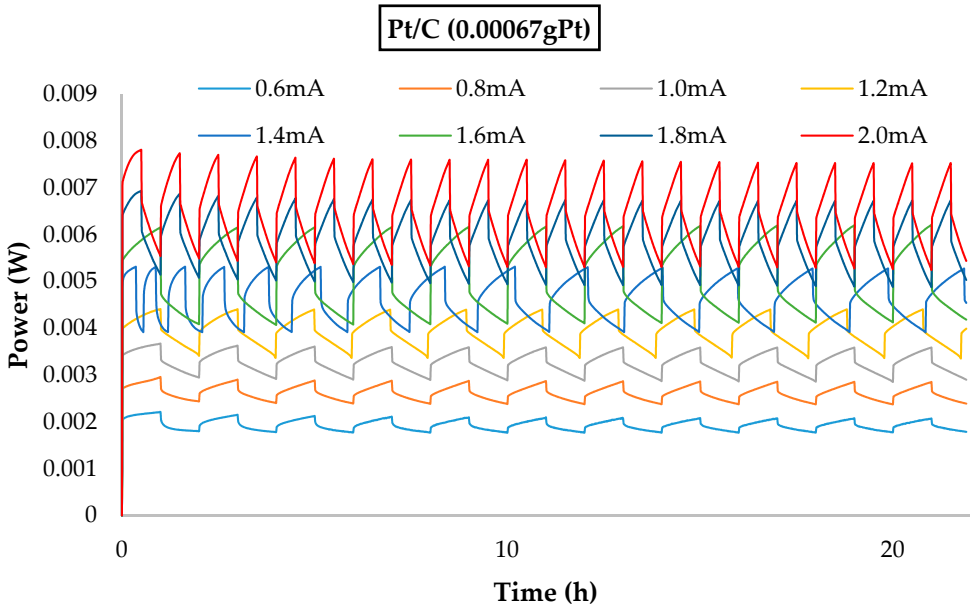


Figure 10. Time evolution of the power obtained after testing the NASICON membrane battery at currents of 0.6, 0.8, 1.0, 1.2, 1.4 1.6, 1.8, and 2.0 mA.

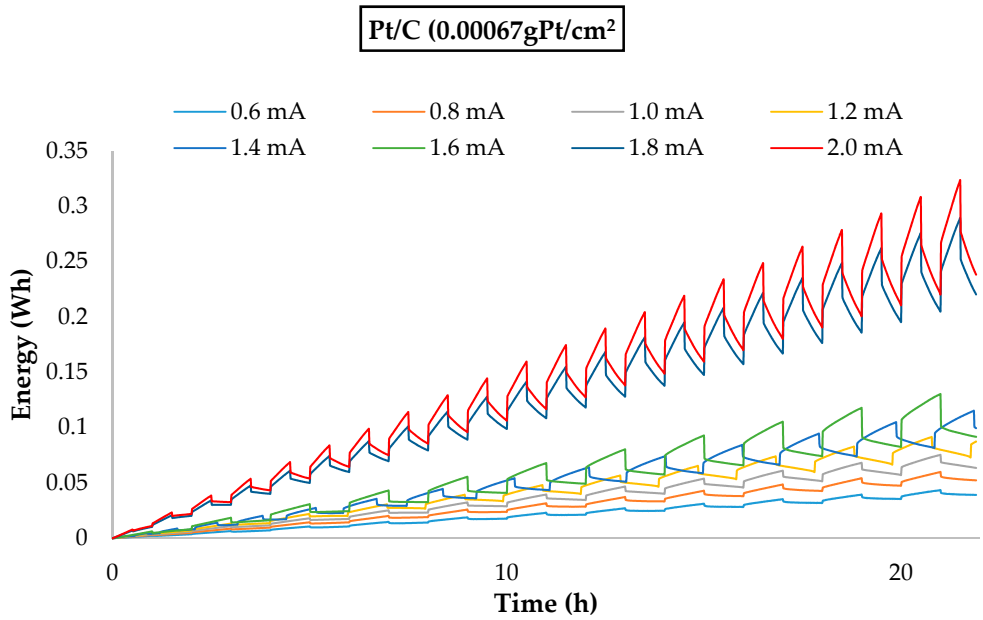


Figure 11. Time evolution of the accumulated energy obtained after testing the NASICON membrane battery at currents of 0.6, 0.8, 1.0, 1.2, 1.4, 1.6, 1.8, and 2.0 mA.

Figure 13 illustrates the charge–discharge curves obtained at different current densities: 0.28, 0.37, 0.47, 0.56, 0.74, 0.84, and 0.93 mA/cm^2, calculated based on the surface of the solid electrolyte. Generally, the charging potential increases with higher current density, while the potential decreases during discharging at higher current densities. Power, energy, and capacity all exhibit an increasing trend during both charging and discharging. Some of the performances of seawater rechargeable batteries found in the literature are shown in Table 3.

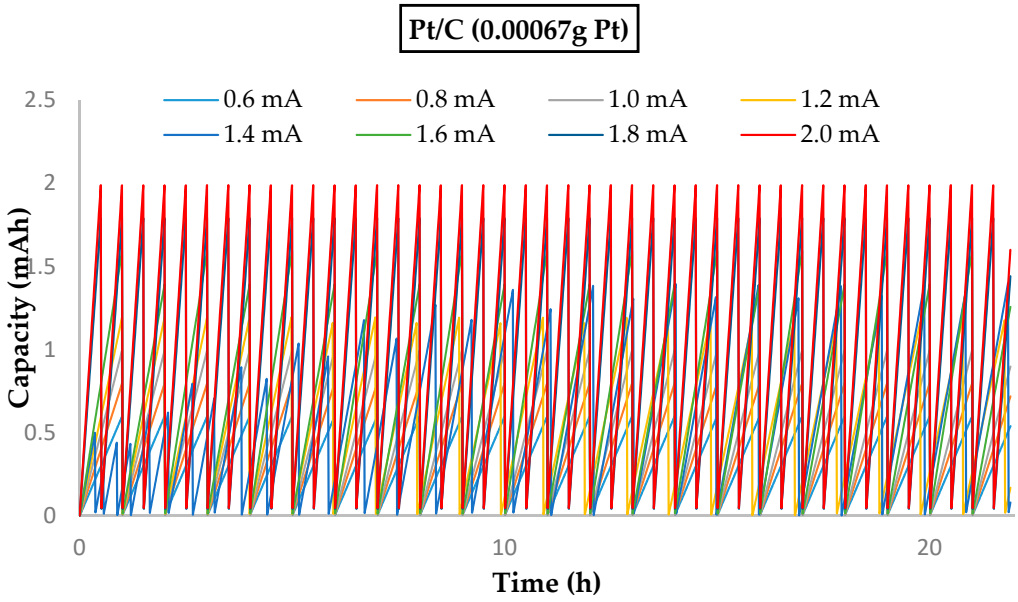


Figure 12. Time evolution of the capacity obtained after testing the NASICON membrane battery at currents of 0.6, 0.8, 1.0, 1.2, 1.4, 1.6, 1.8, and 2.0 mA.

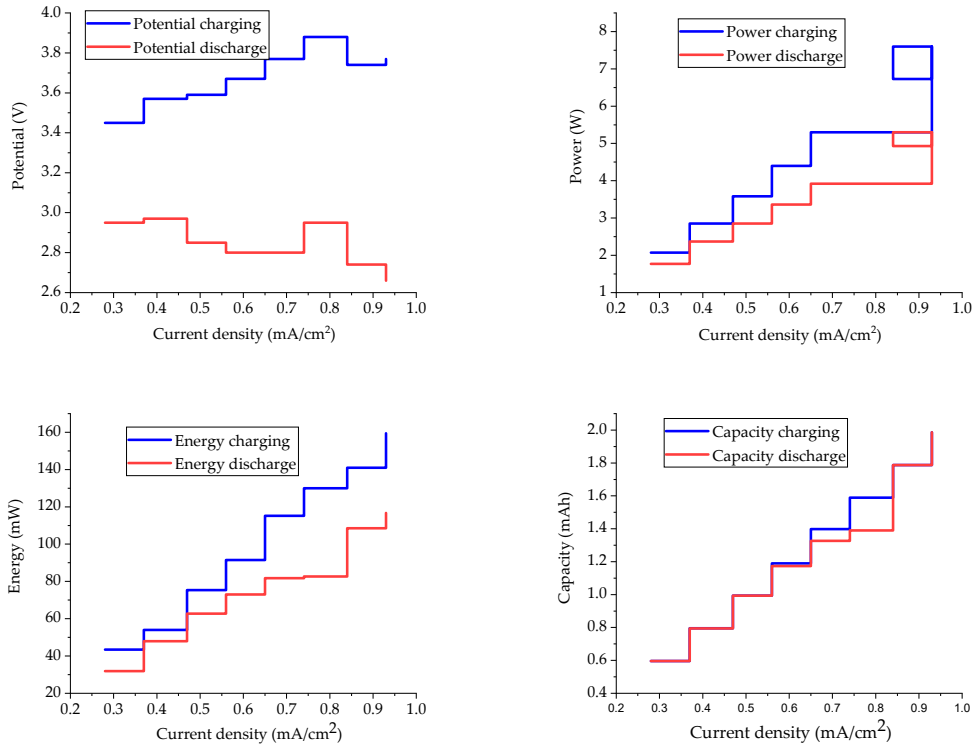


Figure 13. Time evolution of the potential, power, energy and capacity obtained after testing the NASICON membrane battery at current densities of 0.28, 037, 0.47, 0.56, 0.65, 0.74, 0.84, and 0.93 mA/cm^2.

Table 3. Seawater battery performance reported in the literature.

Battery Type	Cycle Time (h)	Current (mA)/(mA/cm^2)	Potential (V)	Capacity Discharge (mAh)/(mAh/g)	Energy Discharge (mWh)/(mAh/g)	Reference
Our SWB	1	0.6/0.28	3.45	1.99/-	116.7/-	[present work]
SWB (coin)	20	0.6/0.28	3.48	67.0/-	118.0	[10]
Li-ion	-	-	3.60	-/273.8	-	[10]
Na-air	-	-	2.33	-/3350.0	-	[10]
Zn-air	-	-	1.66	-/3350.0	-	[10]
Al-air	-	-	2.73	-/3350.0	-	[10]
Na-CO_2	10	0.05/-	3.45	-/500	-	[13]
Na-SWB	6	-/0.025	3.52	-	-	[36]

3.4. Potential Applications of Seawater Activated Batteries and the Future Development Directions of Batteries Activated with Seawater

The charging and discharging processes of rechargeable batteries can be completed in seawater, making them an open cathode system. As a result, these batteries are superior to other batteries in terms of their suitability for marine, offshore, and onshore power sources, as well as energy storage applications. Marine lifejackets can benefit from this type of battery to power a light source and GPS, which can provide location information for anyone in need of assistance in an emergency. These batteries may also be useful in lighthouses, which illuminate objects along the coast and in the open ocean to help ships and boats navigate and warn of obstacles. Seawater batteries can power light beacons to detect obstacles using ultrasonic signals and assess the depth of water. Also, seawater-activated rechargeable batteries on autonomous surface vehicles can provide a constant power source for 24 h of operation. Seawater batteries are available for use in remotely operated vehicles (ROVs) such as underwater robots and drones, both for military and heavy industrial applications and for oceanographic and marine biological research. Another application for seawater-activated batteries is underwater scooters (UWS), which are used for exploring colorful and intricate reefs [34].

Regarding the future development directions of batteries activated with seawater, first of all, the performance of the electrode materials must be optimized. Second, the electrolyte control system needs to be optimized. The performance of seawater-activated batteries depends on the water's temperature, salinity, and flow rate, as they use natural seawater. Controlling and optimizing the electrolytic system is crucial for improving battery performance. Further improving volumetric and gravimetric energy densities requires extensive research on the fabrication of battery platforms and components, as well as the development of cost-effective catalysts. The current use of seawater batteries involves ceramic electrolytes, a method that can be improved by doping them with appropriate cations to improve the Na ion conductivity. Furthermore, maximizing the thickness of these membranes is crucial for the battery's weight and overall durability. Seawater battery power performance, energy efficiency, and cycle stability are greatly influenced by the cathode compartment [8].

4. Conclusions

This study focuses on the preparation and characterization of $Na_{3.0}Zr_2Si_2PO_{12}$- and $Na_{3.15}Zr_2Si_2PO_{12}$-type ceramic membranes and testing their stability in seawater batteries used as solid electrolyte. From the surface analysis, it was observed that the $Na_{3.15}Zr_2Si_2PO_{12}$ powder showed a specific surface area of 2.94 m^2/g compared to 2.69 m^2/g for the $Na_{3.0}Zr_2Si_2PO_{12}$ powder. The measured NASICON samples achieved ionic conductivities between 7.42×10^{-5} and 4.4×10^{-4} S/cm compared to the NASICON commercial membrane with an ionic conductivity of 3.9×10^{-4} S/cm. Battery testing involved charging/discharging at various constant current values (0.6–2.0 mA), using Pt/C as the catalyst and seawater as the catholyte. The electrochemical cell was used to conduct

charge/discharge tests using seawater with a concentration of approximately 20 g Cl^-/L. The seawater was bubbled with CO_2 at a flow rate of 0.5 L/min.

The batteries operated for approximately 20 h, with a discharge capacity ranging from 0.596 to 1.987 mAh and accumulated energy between 32.0 and 116.7 mWh. At a current of 0.6 mA, the discharge/charge potential was observed to be 2.95 V and 3.45 V, respectively, with a potential difference of 0.5 V, and at a current of 2.0 mA, the discharge/charge potential was 2.66 V and 3.77 V, with a potential difference of 1.1 V.

The research determined that rechargeable batteries can undergo charge and discharge processes in seawater, making them an open cathode system. As a result, these batteries are more suitable than others for marine, offshore, and onshore power and energy storage applications. When considering the future development directions of seawater activated batteries, there are three main areas to focus on. First, optimizing the performance of the electrode materials is crucial. Second, it is important to optimize the electrolyte control system. Thirdly, extensive research must be conducted on the fabrication of battery platforms and components, as well as the creation of cost-effective catalysts to further improve volumetric and gravimetric energy.

Author Contributions: Conceptualization M.I. and A.O.; methodology, M.I. and A.O.; investigation, A.M., A.O., G.U. and S.B.; writing—original draft preparation, M.I. and A.O.; writing—review and editing, M.I., A.O. and A.M. The manuscript's published version has been read and agreed to by all authors. All authors have read and agreed to the published version of the manuscript.

Funding: This work was financially supported by project PN 23 15 01 03 and PN 23 15 01 04, Contract No. 20N/2023, financing was provided by the Ministry of Research, Innovation, and Digitization of Romania; project no. 345/2021, 4C-ICSI project, SMIS 125119; project no. 308/2020, HyRo 2.0 project, SMIS 127318.

Data Availability Statement: The article includes the original contributions presented in the study, and any further inquiries can be directed to the corresponding author.

Conflicts of Interest: The authors have declared no conflicts of interest.

References

1. Park, S.; Yoon, N.; Ullah, Z.; Tarus, B.K.; Choi, B.; Kim, H.H.; Son, M. Energy storage capability of seawater batteries for intermittent power generation systems: Conceptualization and modeling. *J. Power Sources* **2023**, *580*, 233322. [CrossRef]
2. Barelli, L.; Pelosi, D.; Bidini, G.; Di Donato, G.; Navarra, M.A.; Passerini, S. Na-seawater battery technology integration with renewable energies: The case study of Sardinia Island. *Renew. Sustain. Energy Rev.* **2023**, *187*, 113701. [CrossRef]
3. Elminshawy, N.A.; Diab, S.; Yassen, Y.E.; Elbaksawi, O. An energy-economic analysis of a hybrid PV/wind/battery energy-driven hydrogen generation system in rural regions of Egypt. *J. Energy Storage* **2024**, *80*, 110256. [CrossRef]
4. Aslam, M.K.; Wang, H.; Chen, S.; Li, Q.; Duan, J. Progress and perspectives of metal (Li, Na, Al, Zn and K)–CO_2 batteries. *Mater. Today Energy* **2023**, *31*, 101196. [CrossRef]
5. Elahi, S.; Seddighi, S. Renewable energy storage using hydrogen produced from seawater membrane-less electrolysis powered by triboelectric nanogenerators. *J. Power Sources* **2024**, *609*, 234682. [CrossRef]
6. Lu, Y.; Yuan, Y.; Liang, T.; Jia, H.; Meng, L.; Zhang, X.; Zhang, S.; Wen, B.; Feng, Z.; Yin, T.; et al. Mechanisms elucidation of secondary seawater batteries: From ion migration to conversion for sustainable energy storage. *Chem. Eng. J.* **2024**, *498*, 155307. [CrossRef]
7. Schär, S.; Bischi, A.; Baccioli, A.; Desideri, U.; Geldermann, J. Optimization of sustainable seawater desalination: Modeling renewable energy integration and energy storage concepts. *Energy Convers. Manag.* **2023**, *293*, 117447. [CrossRef]
8. Chen, J.; Xu, W.; Wang, X.; Yang, S.; Xiong, C. Progress and Applications of Seawater-Activated Batteries. *Sustainability* **2023**, *15*, 1635. [CrossRef]
9. Hwang, S.M.; Park, J.S.; Kim, Y.; Go, W.; Han, J.; Kim, Y.; Kim, Y. Rechargeable seawater batteries—From concept to applications. *Adv. Mater.* **2019**, *31*, 1804936. [CrossRef]
10. Kim, Y.; Harzandi, A.M.; Lee, J.; Choi, Y.; Kim, Y. Design of large-scale rectangular cells for rechargeable seawater batteries. *Adv. Sustain. Syst.* **2021**, *5*, 2000106. [CrossRef]
11. Han, J.; Hwang, S.M.; Go, W.; Senthilkumar, S.T.; Jeon, D.; Kim, Y. Development of coin-type cell and engineering of its compartments for rechargeable seawater batteries. *J. Power Sources* **2018**, *374*, 24–30. [CrossRef]
12. Park, J.; Park, J.S.; Senthilkumar, S.T.; Kim, Y. Hybridization of cathode electrochemistry in a rechargeable seawater battery: Toward performance enhancement. *J. Power Sources* **2020**, *450*, 227600. [CrossRef]

13. Im, E.; Ryu, J.H.; Baek, K.; Moon, G.D.; Kang, S.J. "Water-in-salt" and NASICON Electrolyte-Based Na–CO_2 Battery. *Energy Storage Mater.* **2021**, *37*, 424–432. [CrossRef]
14. Li, Y.; Li, M.; Sun, Z.; Ni, Q.; Jin, H.; Zhao, Y. Recent advance on NASICON electrolyte in solid-state sodium metal batteries. *Energy Storage Mater.* **2023**, *56*, 582–599. [CrossRef]
15. Ignaszak, A.; Pasierb, P.; Gajerski, R.; Komornicki, S. Synthesis and properties of Nasicon-type materials. *Thermochim. Acta* **2005**, *426*, 7–14. [CrossRef]
16. Samiee, M.; Radhakrishnan, B.; Rice, Z.; Deng, Z.; Meng, Y.S.; Ong, S.P.; Luo, J. Divalent-doped $Na_3Zr_2Si_2PO_{12}$ natrium superionic conductor: Improving the ionic conductivity via simultaneously optimizing the phase and chemistry of the primary and secondary phases. *J. Power Sources* **2017**, *347*, 229–237. [CrossRef]
17. Fuentes, R.O.; Figueiredo, F.M.; Marques FM, B.; Franco, J.I. Influence of microstructure on the electrical properties of NASICON materials. *Solid State Ion.* **2001**, *140*, 173–179. [CrossRef]
18. Jolley, A.G.; Taylor, D.D.; Schreiber, N.J.; Wachsman, E.D. Structural investigation of monoclinic-rhombohedral phase transition in $Na_3Zr_2Si_2PO_{12}$ and doped NASICON. *J. Am. Ceram. Soc.* **2015**, *98*, 2902–2907. [CrossRef]
19. Guin, M.; Tietz, F.; Guillon, O. New promising NASICON material as solid electrolyte for sodium-ion batteries: Correlation between composition, crystal structure and ionic conductivity of $Na_{3+x}Sc_2SixP_{3-x}O_{12}$. *Solid State Ion.* **2016**, *293*, 18–26. [CrossRef]
20. Park, H.; Jung, K.; Nezafati, M.; Kim, C.S.; Kang, B. Sodium ion diffusion in Nasicon ($Na_3Zr_2Si_2PO_{12}$) solid electrolytes: Effects of excess sodium. *ACS Appl. Mater. Interfaces* **2016**, *8*, 27814–27824. [CrossRef]
21. Naqash, S.; Ma, Q.; Tietz, F.; Guillon, O. $Na_3Zr_2(SiO_4)_2(PO_4)$ prepared by a solution-assisted solid-state reaction. *Solid State Ion.* **2017**, *302*, 83–91. [CrossRef]
22. Jalalian-Khakshour, A.; Phillips, C.O.; Jackson, L.; Dunlop, T.O.; Margadonna, S.; Deganello, D. Solid-state synthesis of NASICON ($Na_3Zr_2Si_2PO_{12}$) using nanoparticle precursors for optimisation of ionic conductivity. *J. Mater. Sci.* **2020**, *55*, 2291–2302. [CrossRef]
23. Ruan, Y.; Guo, F.; Liu, J.; Song, S.; Jiang, N.; Cheng, B. Optimization of $Na_3Zr_2Si_2PO_{12}$ ceramic electrolyte and interface for high performance solid-state sodium battery. *Ceram. Int.* **2019**, *45*, 1770–1776. [CrossRef]
24. Xiang, L.; Li, X.; Xiao, J.; Zhu, L.; Zhan, X. Interface issues and challenges for NASICON-based solid-state sodium-metal batteries. *Adv. Powder Mater.* **2024**, *3*, 100181. [CrossRef]
25. Yang, J.; Wan, H.L.; Zhang, Z.H.; Liu, G.Z.; Xu, X.X.; Hu, Y.S.; Yao, X.Y. NASICON-structured $Na_{3.1}Zr_{1.95}Mg_{0.05}Si_2PO_{12}$ solid electrolyte for solid-state sodium batteries. *Rare Met.* **2018**, *37*, 480–487. [CrossRef]
26. Li, X.; Zhou, Q.; Wu, J.; Yuan, C.; Lu, K.; Zhan, X.; Zhu, L. An in Situ Formed Multifunctional Interphase with High Dendrite Tolerance for Long-Life Solid-State Sodium–Metal Batteries. *ACS Appl. Energy Mater.* **2023**, *6*, 10333–10339. [CrossRef]
27. Liu, Y.; Fu, H.; Gao, C.; Wen, J.; Guo, R.; Luo, W.; Zhou, J.; Lu, B. Solvation Structure Dual-Regulator Enabled Multidimensional Improvement for Low-Temperature Potassium Ion Batteries. *Adv. Energy Mater.* **2024**, 2403562. [CrossRef]
28. Wen, J.; Fu, H.; Zhang, D.; Ma, X.; Wu, L.; Fan, L.; Yu, X.; Zhou, J.; Lu, B. Nonfluorinated antisolvents for ultrastable potassium-ion batteries. *ACS Nano* **2023**, *17*, 16135–16146. [CrossRef]
29. Shi, Y.; Peng, C.; Feng, Y.; Wang, R.; Wang, N. Microstructure and electrochemical corrosion behavior of extruded Mg–Al–Pb–La alloy as anode for seawater-activated battery. *Mater. Des.* **2017**, *124*, 24–33. [CrossRef]
30. Kim, C.; Kim, J.; Joo, S.; Bu, Y.; Liu, M.; Cho, J.; Kim, G. Efficient CO_2 utilization via a hybrid Na-CO_2 system based on CO_2 dissolution. *iScience* **2018**, *9*, 278–285. [CrossRef]
31. Wang, W.; Yuan, W.; Zhao, Z.; Zou, D.; Zhang, P.; Shi, Z.; Weng, J.; Zhou, P. Enhanced ionic conductivity of Cu-doped NASICON solid electrolyte for solid-state sodium batteries. *J. Electroanal. Chem.* **2023**, *937*, 117405. [CrossRef]
32. Oh, J.A.S.; Wang, Y.; Zeng, Q.; Sun, J.; Sun, Q.; Goh, M.; Chua, B.; Zeng, K.; Lu, L. Intrinsic low sodium/NASICON interfacial resistance paving the way for room temperature sodium-metal battery. *J. Colloid Interface Sci.* **2021**, *601*, 418–426. [CrossRef] [PubMed]
33. Iordache, M.; Oubraham, A.; Petreanu, I.; Sisu, C.; Borta, S.; Capris, C.; Soare, A.; Marinoiu, A. NASICON Membrane with High Ionic Conductivity Synthesized by High-Temperature Solid-State Reaction. *Materials* **2024**, *17*, 823. [CrossRef] [PubMed]
34. Iordache, M.; Oubraham, A.; Borta, S.; Marinoiu, A. The Chemical Stability of NASICON Solid Electrolyte for Seawater Batteries. In Proceedings of the 2024 16th International Conference on Electronics, Computers and Artificial Intelligence (ECAI), Iasi, Romania, 27–28 June 2024; IEEE: Piscataway, NJ, USA, 2024; pp. 1–6.
35. Zhang, X.; Wang, J.; Wen, J.; Wang, Y.; Li, N.; Wang, J.; Fan, L. Improvement of ionic conductivity and densification of $Na_3Zr_2Si_2PO_{12}$ solid electrolyte rapidly prepared by microwave sintering. *Ceram. Int.* **2022**, *48*, 18999–19005. [CrossRef]
36. Zhang, Y.; Park, J.S.; Senthilkumar, S.T.; Kim, Y. A novel rechargeable hybrid Na-seawater flow battery using bifunctional electrocatalytic carbon sponge as cathode current collector. *J. Power Sources* **2018**, *400*, 478–484. [CrossRef]

Disclaimer/Publisher's Note: The statements, opinions and data contained in all publications are solely those of the individual author(s) and contributor(s) and not of MDPI and/or the editor(s). MDPI and/or the editor(s) disclaim responsibility for any injury to people or property resulting from any ideas, methods, instructions or products referred to in the content.